Biosensors and Bioelectronics 52 (2014) 209–215

Contents lists available at ScienceDirect

Biosensors and Bioelectronics

journal homepage: www.elsevier.com/locate/bios

Copper, zinc superoxide dismutase and nitrate reductase coimmobilized bienzymatic biosensor for the simultaneous determination of nitrite and nitrate

Thangamuthu Madasamy [a], Manickam Pandiaraj [a], Murugesan Balamurugan [a], Kalpana Bhargava [b], Niroj Kumar Sethy [b], Chandran Karunakaran [a,*]

[a] Biomedical Research Laboratory, Department of Chemistry, VHNSN College (Autonomous), Virudhunagar 626001, Tamil Nadu, India
[b] Peptide and Proteomics Division, DIPAS, DRDO, Delhi 110054, India

ARTICLE INFO

Article history:
Received 13 May 2013
Received in revised form
5 August 2013
Accepted 6 August 2013
Available online 28 August 2013

Keywords:
Bienzymatic biosensor
Copper, zinc superoxide dismutase
Nitrate reductase
Simultaneous determination
Nitrite
Nitrate

ABSTRACT

This work presents a novel bienzymatic biosensor for the simultaneous determination of nitrite (NO_2^-) and nitrate (NO_3^-) ions using copper, zinc superoxide dismutase (SOD1) and nitrate reductase (NaR) coimmobilized on carbon nanotubes (CNT)–polypyrrole (PPy) nanocomposite modified platinum electrode. Morphological changes of the PPy and CNT modified electrodes were investigated using scanning electron microscopy. The electrochemical behavior of the bienzymatic electrode (NaR–SOD1–CNT–PPy–Pt) was characterized by cyclic voltammetry exhibiting quasi-reversible redox peak at +0.06 V and reversible redox peaks at −0.76 and −0.62 V vs. Ag/AgCl, for the immobilized SOD1 and NaR respectively. The electrocatalytic activity of SOD1 towards NO_2^- oxidation observed at +0.8 V was linear from 100 nM to 1 mM with a detection limit of 50 nM and sensitivity of 98.5 ± 1.7 nA μM^{-1} cm^{-2}. Similarly, the coimmobilized NaR showed its electrocatalytic activity towards NO_3^- reduction at −0.76 V exhibiting linear response from 500 nM to 10 mM NO_3^- with a detection limit of 200 nM and sensitivity of 84.5 ± 1.56 nA μM^{-1} cm^{-2}. Further, the present bienzymatic biosensor coated with cellulose acetate membrane for the removal of non-specific proteins was used for the sensitive and selective determinations of NO_2^- and NO_3^- present in human plasma, whole blood and saliva samples.

1. Introduction

Nitric oxide (NO) is an essential messenger molecule regulating the biological processes viz. blood vessel relaxation, neuronal cell-to-cell communication and immune function. (Bredt and Snyder, 1994; Lowenstein et al., 1994). Due to the rapid metabolism and short half-life time of NO, it is readily oxidized into its metabolites nitrite (NO_2^-) and nitrate (NO_3^-) (Szabo, 1996). Therefore, the NO level is commonly assessed by determining plasma concentrations of NO_2^- and NO_3^- or that of total NO_x ($NO_2^- + NO_3^-$) (Vitturi and Patel, 2011). Further, NO_2^- and NO_3^- are recently emerged as an endocrine reservoir capable of producing NO within hypoxic, ischemic or injured tissue (Lundberg et al., 2008, Lundberg et al., 2009). More prominently, the blood concentrations of NO_2^- and NO_3^- are possibly altered in physiological hypoxic signaling, vasodilation, modulation of cellular respiration and cellular response to ischemic stress (Kevil and Lefer, 2011; Butler and Feelisch, 2008). Hence, the measurements of NO_2^- and NO_3^- are imperative in human physiology as it provides valuable information with regard to in vivo NO production, bioavailability and prognostic of various diseases including oxidative stress. Moreover, determinations of NO_2^- and NO_3^- ions are also important in environmental pollution, agriculture, marine cycles, water management and food analysis.

Numerous strategies have been reported for the determination of NO_2^- and NO_3^- including the Griess colorimetric assay (Guevara et al., 1998; Miranda et al., 2001; Nataliya and Andrei, 2005), fluorometry (Fang et al., 2009) and chemiluminescence methods (Nagababu and Rifkind, 2010). Separation based methods viz. GC–MS (Tsikas et al., 2012; Kage et al., 2002) and HPLC (Jobgen et al., 2007) with variety of detection system have also been reported. Based on the spectrophotometric determination, some commercial assay kits are also available in the market (Sigma, Catalog no. 06239; Cayman Chemical Company, Prod. no. 850-001-KI01). Most of these techniques are indirect, not suitable for in vivo measurement and require sophisticated instruments. Usually, they have tedious detection procedures and therefore are time-consuming. Recently, electrochemical biosensor techniques are proved to be a powerful tool for the measurement of NO_2^- and NO_3^- by providing practical advantages, such as operation simplicity, low expense of fabrication and suitability

* Corresponding author. Tel.: +91 04562 280154; fax: +91 04562 281338.
E-mail addresses: ckaru2000@gmail.com, ckaru2000@yahoo.com (C. Karunakaran).

0956-5663/$ - see front matter © 2013 Elsevier B.V. All rights reserved.
http://dx.doi.org/10.1016/j.bios.2013.08.036

for real-time detection. In addition, it provides fast response, more sensitive (particularly with the use of modified electrodes) and selective determination.

In the literature, several electrochemical biosensors were reported for the independent determinations of NO_2^- and NO_3^- (Badea et al., 2001; Boo et al., 2007; Gamboa et al., 2009; Geng et al., 2008; Quan et al., 2005; Rocha et al., 2002; Sohail and Adeloju, 2008; Sun and Wang, 2009; Wang et al., 2006; Zhang et al., 2009). Recently, there has been emergent interest in the direct determination of NO_2^- and NO_3^- simultaneously without any separation steps to save time and cost of the experiments. In this exertion, researchers have developed the electrochemical sensors for the simultaneous determination of NO_2^- and NO_3^- using silver-doped zeolite (Manea et al., 2010), copper complex (Shiddiky et al., 2006), graphite (Kaminskaya et al., 2004) and copper electrodes (Shariar and Hinoue, 2010). However, non-selectivity of these chemically modified electrodes limited their applications to biological samples for the reason that the co-existing biological substrates probably interfere with the measurement and also the concentrations of NO_2^- and NO_3^- are in low molar level. Moreover, its operation under normal physiological conditions is also uncertain. Therefore, there is a real need for the simultaneous measurement of NO_2^- and NO_3^- in biological samples with high specificity and sensitivity.

In order to overcome these limitations, for the first time we have developed here a novel bienzymatic biosensor system for the simultaneous determination of NO_2^- and NO_3^- using copper, zinc superoxide dismutase (SOD1) and nitrate reductase (NaR) coimmobilized electrode. It is based on our previous research works for the independent determinations of NO_2^- using SOD1 (Rajesh et al., 2010) and NO_3^- using NaR modified electrodes (Madasamy et al., 2013). The stable coimmobilization of two enzymes on an electrode surface with complete retention of its biological activity is a crucial problem for the development of biosensors. The electrode surface modified with polypyrrole (PPy) provides porous host matrix for the immobilization of SOD1 and NaR. It also affords well-ordered conductive polymer chain with good environmental stability (Reiter et al., 2001). Further, modification of PPy matrix with carbon nanotubes (CNT) forms CNT–PPy nanocomposite which access additional surface area to immobilize more SOD1 and NaR and also act as molecular wires to accelerate electron transfer between underlying electrode and active sites thereby increasing the sensitivity of the biosensor. Further, to eliminate all the possible interferences during the NO_2^- and NO_3^- measurements in biological samples, cellulose acetate (CA) membrane was used. The analytical applicability of this highly sensitive and selective bienzymatic biosensor was investigated for human plasma, whole blood and saliva samples under normal physiological conditions.

2. Materials and methods

2.1. Chemicals and reagents

Copper, zinc superoxide dismutase from bovine erythrocytes, nitrate reductase from *Aspergillus niger*, cellulose acetate, acetone, sodium ascorbate, uric acid, sodium hydrogen phosphate, disodium hydrogen phosphate, pyrrole, $NaNO_3$, $NaNO_2$, KCl and glutaraldehyde were purchased from Sigma Company (Milwaukee, WI, USA). Single walled carbon nanotubes were purchased from carbon solutions Inc., CA, USA. All the solutions were prepared with doubly distilled water.

2.2. Preparation of Human plasma, Blood and saliva samples

The protocol for the collection of human saliva and blood was approved by the Institutional ethical committee. A written informed consent was obtained from the donors before salivary and blood collection. A total of six healthy male volunteers (23–28 years) were recruited for the study. All the participants were free from fever, cold, non-smokers and had good oral hygiene. The saliva samples were collected between 9 am and 11 am and the participants were asked to refrain from eating and drinking one hour prior to saliva collection. The participants rinsed their mouth with water prior to collection, and waited 10 min before commencing with the collection. Resting drooling (minimal oral movements) method was used to collect whole mouth saliva from the oral cavity. Participants were asked to sit comfortably in an upright position and tilt their heads down slightly to pool saliva in the mouth. The first expectoration was discarded to eliminate food debris and unwanted substance contaminating the sample that may cause analytical inaccuracy. The subsequent sample was then expectorated into a pre-labelled sterile container. Around 2 mL saliva was collected and stored at −80 °C. All the stored salivary samples were subjected to freeze-thaw cycles to break down mucopolysaccharides to reduce viscosity and to minimize pipetting errors. All thawed saliva samples were centrifuged at 10,000*g* for 10 min at 4 °C to remove cellular debris and to minimize the salivary turbidity which can negatively impact on the accuracy of analysis (Worthman et al., 1990; Schipper et al., 2007; Mohamed et al., 2012). Blood was drawn by standard venipuncture into 4 ml Vacutainer tubes using EDTA as anticoagulant (BD Worldwide, NJ, USA). Plasma was obtained by centrifugation of whole blood for 15 min at 380*g*. The plasma samples were passed through 10 kDa cutoff membranes and further used for nitrate/nitrite estimation.

2.3. Instrumentations

All the electrochemical experiments were performed using CHI 1200B electrochemical workstation (CHI, USA) with a conventional three electrode system which consisted of an Ag/AgCl wire as reference electrode, a Pt wire as auxiliary or counter electrode and a Pt electrode with SOD1 and NaR coimmobilized on CNT–PPy nanocomposite as working electrode. The size of Pt wire working electrode was 0.5 mm in diameter. The morphological images were obtained using a FEI Quanta FEG 200-High Resolution Scanning Electron Microscope (FEI Co., Netherlands).

2.4. Construction of bienzymatic (NaR–SOD1–CNT–PPy–Pt) biosensor

CNT modified PPy–Pt electrode was constructed as per our earlier report (Madasamy et al., 2012). Briefly, pyrrole was electropolymerized onto the Pt electrode by the irreversible oxidation of 0.4 M pyrrole in 0.1 M KCl as supporting electrolyte by applying potential from 0 V to 0.9 V vs. Ag/AgCl at a scan rate of 50 mV s^{-1} for 10 complete cycles. Then, CNT integrated PPy–Pt electrode was made by dropping 25 μL of CNT solution (1 ml of 0.5 wt% nafion–ethanol solution containing 2 mg of CNT) onto the PPy–Pt electrode and dried at room temperature. The enzyme solutions were prepared in 0.1 M PBS (pH 7.0) with working concentration of 300 U/ml for SOD1 and 10 U/ml for NaR. Then, these enzyme solutions were mixed in the ratio of 1:1 and 10 μL of the mixture was dropped onto the CNT–PPy–Pt electrode by employing 5 μL of glutaraldehyde as a cross-linking agent. During this process, SOD1 and NaR were coimmobilized on CNT–PPy–Pt electrode. Further, it was immersed in 0.1 M PBS to remove loosely affixed SOD1/NaR and dried at room temperature, stored at 4 °C when not in use. The above fabricated bienzymatic biosensor is represented in Scheme 1.

3. Results and discussion

In a single experiment, measurement of various analytes using multienzymatic biosensor is a challenging research area. Asav et al.

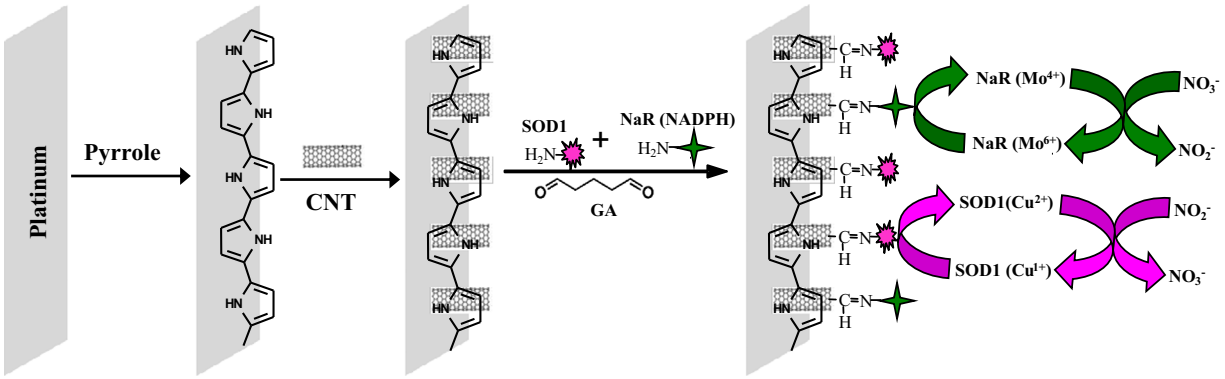

Scheme 1. Schematic representation of the construction of NaR–SOD1–CNT–PPy–Pt electrode and illustration of reactions during the simultaneous determination of NO_2^- and NO_3^-..

developed a bienzymatic biosensor for the simultaneous determination of alcohol and glucose using alcohol oxidase and glucose oxidase coimmobilized electrode (Asav and Akyilmaz, 2010). Similarly, a bienzymatic biosensor for the simultaneous determination of glucose and fructose was also reported (Campuzano et al., 2004). As mentioned earlier, the measurements of NO_2^- and NO_3^- are very important in biology, nutrition and therapeutics (Lundberg et al., 2009) and are challenging due to their low concentrations in biological samples. Therefore, a highly sensitive and specific bienzymatic biosensor system for the simultaneous measurement of NO_2^- and NO_3^- has been developed and reported. It is based on the electrochemical oxidation of NO_2^- by SOD1 and reduction of NO_3^- using NaR. Based on our earlier findings (Pandiaraj et al., 2013), the CNT–PPy nanocomposite was used here as a host matrix for the coimmobilization of SOD1 and NaR to enhance the sensitivity of the biosensor. The analytical performance and utility of the proposed bienzymatic biosensor was investigated and optimized.

3.1. Morphological characterization of the electrodes

Fig. 1A(a), (b), and (c) illustrates the scanning electron microscopic (SEM) images of bare Pt, PPy–Pt and CNT–PPy–Pt electrodes respectively. Fig. 1A(b) reveals the typical highly porous morphology of PPy on Pt electrode surface. This high porous background of PPy perhaps provides much larger surface area to bind more CNT and hence SOD1/NaR at the electrode surface. Further, Fig. 1A(c) shows the integration of CNT in the PPy matrix. Moreover, the distribution of CNT on PPy also confirmed using energy dispersive x-ray analysis spectrum as shown in Fig. S1.

3.2. Electrochemical characterization

Fig. 1B shows the electrochemical responses obtained for the bare Pt (curve a), PPy–Pt (curve b), CNT–PPy–Pt (curve c) and NaR–SOD1–CNT–PPy–Pt (curve d) electrodes at a scan rate of 50 mV s^{-1} in 0.1 M PBS (pH 7.0). Fig. S2 exhibits the wider potential window CVs of Fig. 1B. The broad peaks were observed in the CV range of −0.8 V to 0.2 V for the PPy–Pt and CNT–PPy–Pt electrodes possibly due to the complex redox features of PPy (Zhu et al., 2009) and high capacitive currents (Wang et al., 2007). However, the CV of SOD1 and NaR coimmobilized on CNT–PPy–Pt electrode exhibits the quasi-reversible redox peak at +0.06 V and reversible redox peaks at −0.76 and −0.62 V vs. Ag/AgCl. These peaks are characteristics of SOD1 (Rajesh et al., 2010) and NaR (Madasamy et al., 2013) respectively. Also, the capacitive current of the bienzymatic electrode was decreased. It is perhaps due to the formation of proteinaceous layer onto the CNT–PPy–Pt electrode surface.

Further, the effective surface coverage of SOD1 and NaR were estimated separately using electrochemical oxidation of NO_2^- and reduction of NO_3^- by applying the Randles–Sevcik equation.

$$I_p = (2.69 \times 10^5) A n^{3/2} D^{1/2} C \gamma^{1/2} \quad (1)$$

where, C and D are the concentration and diffusion coefficient respectively. I_p is the maximum current response, n is the number of electron transferred, γ is the scan rate and A is the effective surface area. The surface coverage of 32.5×10^{-8} mol cm^{-2} for SOD1 and 20×10^{-8} mol cm^{-2} for NaR was obtained. It reveals that the enzymes were effectively loaded on the CNT–PPy nanocomposite modified Pt electrode.

3.3. The influence of pH and scan rate

The electrochemical performance of SOD1 and NaR coimmobilized electrode (NaR–SOD1–CNT–PPy–Pt) was investigated in the pH range of 3.0–10.0. For the pH study, a mixture of disodium hydrogen phosphate and citric acid buffer was used. The increase of pH from 7.0–10.0 and decrease from 7.0–3.0 led to decrease in the current response, indicating that the electrocatalytic response was controlled by the activity of the enzymes. The decrease in current response at low and high pHs is perhaps due to the denaturation of the SOD1 and NaR. As reported earlier, for the independent SOD1 (Madasamy et al., 2012) and NaR (Madasamy et al., 2013) modified electrodes, the bienzymatic electrode also showed maximum activity at pH 7.0 (Fig. S3). Therefore, the present biosensor is more appropriate for the NO_2^- and NO_3^- measurements in biological samples under normal physiological conditions. Further, the influence of scan rate on the electrochemical oxidation of NO_2^- and reduction of NO_3^- at the NaR–SOD1–CNT–PPy–Pt electrode was investigated using cyclic voltammetry to acquire information about electrochemical mechanism. It was found that the anodic peak currents negatively increased for NO_2^- oxidation and cathodic peak currents positively increased for NO_3^- reduction linearly with increasing the scan rate from 50 to 300 mV s^{-1} but the characteristic of CV remains unchanged (Fig. S4). This linear variations of anodic and cathodic peak currents (I_P) with scan rate $(\gamma)^{1/2}$ indicate that the electrochemical process is diffusion controlled (Wang, 2006).

3.4. Electrochemical response to NO_2^-

Fig. 2a displays the electrochemical responses obtained for the NaR–SOD1–PPy–Pt and NaR–SOD1–CNT–PPy–Pt electrodes in the absence (curves a and b) and presence (curves c and d) of 200 μM NO_2^- at a scan rate of 50 mV s^{-1} in 0.1 M PBS (pH 7.0). Before the addition of NO_2^-, there was no change observed in the current response. However, after the addition of 200 μM NO_2^-, NaR–SOD1–PPy–Pt and NaR–SOD1–CNT–PPy–Pt electrodes exhibited the

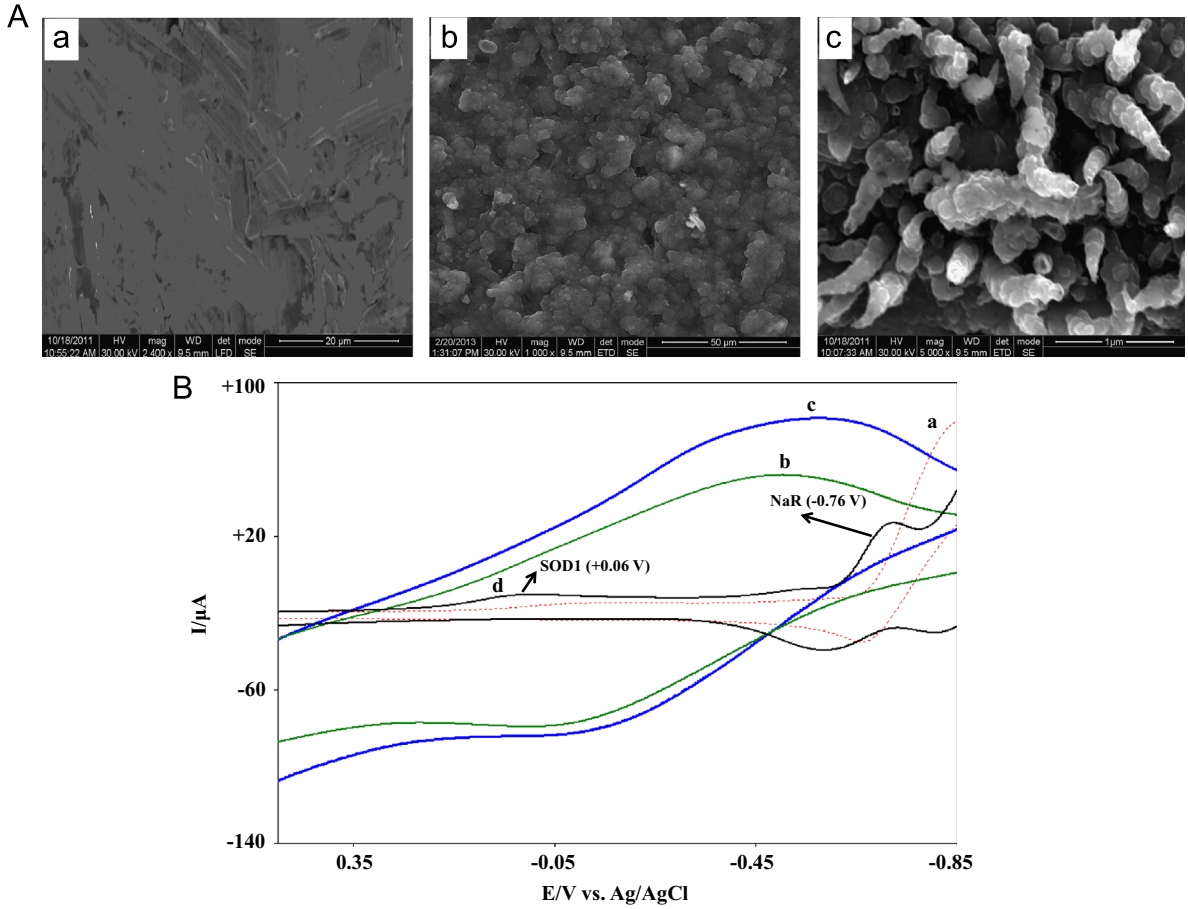

Fig. 1. (A) SEM micrographs of (a) bare Pt, (b) PPy–Pt and (c) CNT–PPy–Pt electrodes. (B) Typical CV responses obtained for the (a) bare Pt, (b) PPy–Pt, (c) CNT–PPy–Pt and (d) NaR–SOD1–CNT–PPy–Pt electrodes in 0.1 M PBS (pH 7.0) at scan rate: 50 mV s^{-1} vs. Ag/AgCl.

significant increases in current anodically at the potential, +0.8 V. It is ascribed to the electrochemical oxidation of NO_2^- to NO_3^- *via* a cyclic redox reaction of SOD1 active site Cu(I/II) moiety. Further, it is obviously seen that the NaR–SOD1–CNT–PPy–Pt electrode (curve d) shows 15 μA higher current than NaR–SOD1–PPy–Pt (curve c). It is perhaps due to the additional surface area provided by the CNT–PPy nanocomposite enhancing the immobilization of SOD1 as well as accelerating electron transfer between underlying electrode and the active site of SOD1.

The electrochemical responses of the NaR–SOD1–CNT–PPy–Pt electrode in 0.1 M PBS (control) and various NO_2^- concentrations using the same scan rate are shown in Fig. S5. As the concentration increases, the anodic current response is also increases linearly at +0.8 V. The observed anodic peak currents vs. NO_2^- concentrations were plotted as shown in the inset of Fig. S5. The calibration curve thus obtained exhibits a linear range of response over the concentration of NO_2^- from 100 nM to 1 mM but for clarity here we have shown from 50 μM to 500 μM (r^2=0.9953 and n=3) with a detection limit of 50 nM and the sensitivity of 98.5 ± 1.7 nA μM^{-1} cm^{-2}.

3.5. *Electrochemical response to* NO_3^-

Fig. 2b illustrates the CV of NaR–SOD1–PPy–Pt and NaR–SOD1–CNT–PPy–Pt electrodes in the absence (curves a and b) and presence (curves c and d) of 400 μM NO_3^- at a scan rate of 50 mV s^{-1} in 0.1 M PBS (pH 7.0). Before the addition of NO_3^-, there was no change observed in the current response. However, after the addition of NO_3^-, NaR–SOD1–PPy–Pt and NaR–SOD1–CNT–PPy–Pt electrodes exhibited the significant increases in current cathodically at the potential, −0.76 V. It is attributed to the reduction of NO_3^- to NO_2^- *via* a cyclic redox reaction of NaR active site Mo(IV/VI) moiety. Further, it is observed here that the NaR–SOD1–CNT–PPy–Pt electrode exhibited 12 μA higher current than the NaR–SOD1–PPy–Pt. Fig. S6 represents the typical CV responses obtained for the NaR–SOD1–CNT–PPy–Pt electrode in the presence of various NO_3^- concentrations at the same scan rate. The observed cathodic peak currents vs. NO_3^- concentrations were plotted as depicted in inset of Fig. S6. The calibration curve obtained exhibits a linear range of response over the concentration of NO_3^- from 500 nM to 10 mM (r^2=0.9995 and n=3) with a detection limit of 200 nM and the sensitivity of 84.5 ± 1.56 nA μM^{-1} cm^{-2}.

3.6. *Simultaneous determination of* NO_2^- *and* NO_3^-

Fig. 3a shows the CVs obtained for the bienzymatic biosensor by increasing the concentration of NO_2^- from 500 nM to 300 μM and NO_3^- from 700 nM to 400 μM at a scan rate of 50 mV s^{-1} in 0.1 M PBS (pH 7.0). The observed results exhibit the increase of well-distinguished anodic peak at +0.8 V and cathodic peak at −0.76 V. The mechanism for the simultaneous measurement of NO_2^- and NO_3^- using the proposed bienzymatic biosensor was based on the nitrite oxidase activity of SOD1 (Rajesh et al., 2010) and nitrate reduction activity of NaR (Madasamy et al., 2013) as follows:

$$SOD1-Cu(II)+NO_2^-+H_2O \rightarrow SOD1-Cu(I)+NO_3^-+2H^++2e^- \quad (2)$$

$$NaR-Mo(IV)+NO_3^- \rightarrow [NaR-Mo(IV)-NO_3^-] \quad (3)$$

$$[NaR-Mo(IV)-NO_3^-]+2H^+ \rightarrow NaR-Mo(VI)+NO_2^-+H_2O \quad (4)$$

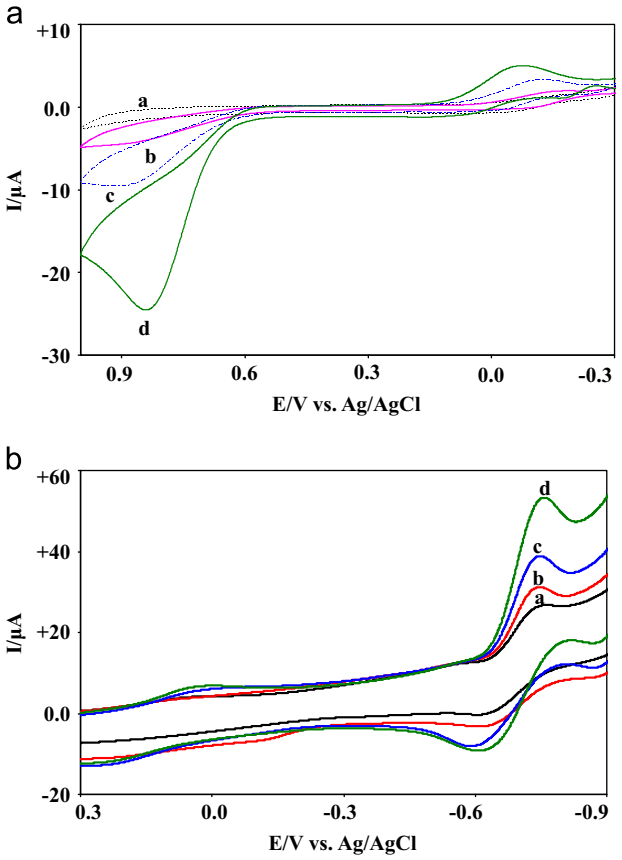

Fig. 2. Electrochemical responses obtained for the NaR–SOD1–PPy–Pt and NaR–SOD1–CNT–PPy–Pt electrodes in the (a) absence (curves a and b) and presence (curves c and d) of 200 μM NO_2^- and (b) absence (curves a and b) and presence of (curves c and d) 400 μM NO_3^- solution in 0.1 M PBS (pH 7.0) at scan rate: 50 mV s^{-1} vs. Ag/AgCl.

$$NaR-Mo(VI)+\beta-NAD(P)H \rightarrow NaR-Mo(IV)+\beta-NAD(P) \quad (5)$$

The calibration curve obtained for the simultaneous measurement of NO_2^- ($r^2=0.999$) and NO_2^- ($r^2=0.995$) is shown in Fig. 3b. Further, the analytical characteristics such as sensitivity and linear range of the present bienzymatic biosensor were compared with the earlier reported NO_2^- and NO_3^- biosensors (Table S1). These results indicate that the NaR–SOD1–CNT–PPy–Pt electrode can be successfully used for the simultaneous measurement of NO_2^- and NO_3^-.

3.7. Selectivity study

Since the oxidation potential of NO_2^- is high, other electroactive species such as ascorbic acid (AsA) and uric acid (UA) present in the biological samples (complex media) can also be oxidized and thus interfere with the NO_2^- measurement. Upon addition of 250 μM UA into 0.1 M PBS containing 100 nM NO_2^- and 300 nM NO_3^-, no current change was observed in time vs. current response of the NaR–SOD1–CNT–PPy–Pt electrode (Fig. S7). Therefore, it did not interfere with the measurement. However, noticeable current change was observed upon addition of 250 μM AsA (Fig. S8, curve b). Earlier, it has been reported that CA membrane was permselective for NO_2^- and NO_3^- (Badea et al., 2001). Therefore, in the present study we have also used CA membrane to eliminate AsA and other possible interferences. CA membrane coated bienzymatic biosensor was prepared by dropping 10 μL of cellulose acetate solution (cellulose acetate in acetone) onto the NaR–SOD1–CNT–PPy–Pt electrode and dried at room temperature. After CA membrane coating, again the similar time vs. current response

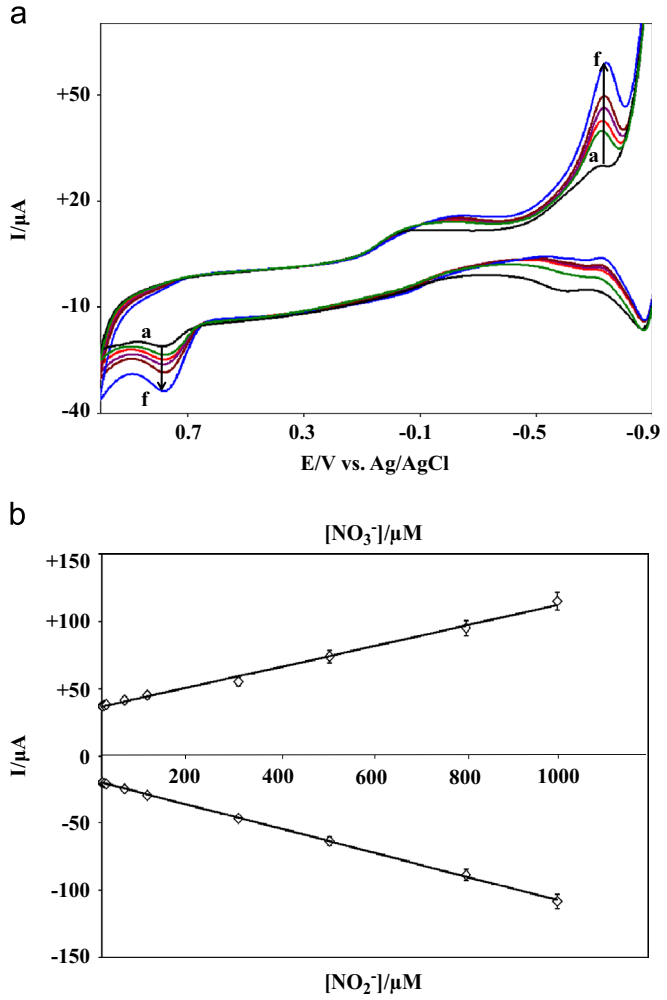

Fig. 3. (a) Typical CV responses obtained for the NaR–SOD1–CNT–PPy–Pt electrode in (a) 500 nM NO_2^- +700 nM NO_3^-, (b) 10 μM NO_2^- +30 μM NO_3^-, (c) 30 μM NO_2^- +50 μM NO_3^-, (d) 50 μM NO_2^- +100 μM NO_3^-, (e) 100 μM NO_2^- +200 μM NO_3^- and (f) 300 μM NO_2^- +400 μM NO_3^- solution at scan rate: 50 mV s^{-1} vs. Ag/AgCl. (b) A linear calibration plot of anodic peak currents against NO_2^- concentrations ($y=-0.087x-19.96$ and $r^2=0.999$) and cathodic peak currents against NO_3^- concentrations ($y=0.075x+36.77$ and $r^2=0.995$).

of the bienzymatic biosensor was investigated in the presence of 250 μM AsA and found that there was no change in current (Fig. S8, curve a). CA membrane not only excludes interferences but also prevents the bienzymatic electrode from fouling due to the non-specific adsorption of proteins (vide infra) and other materials typically present in the biological samples.

3.8. Stability, repeatability and reproducibility

The stability of the NaR–SOD1–CNT–PPy–Pt electrode was evaluated by monitoring the current response thrice a day in the presence of 100 nM NO_2^- and 300 nM NO_3^- over 4 weeks and rest of the time it was stored at 4 °C. The SOD1 and NaR were quite stable inferred from their electrocatalytical activities 92% and 89.6% respectively after 1 month storage and 83% and 76% respectively after 2 month storage. Repeatability of the bienzymatic biosensor was tested by measuring the decrease in current response during five successive CV measurements of NO_2^- and NO_3^-. The resulting standard deviations were 1.2% and 1.5% for NO_2^- and NO_3^-, respectively. Further, to ascertain the reproducibility of the experimental results, four different bienzymatic electrodes were constructed and tested towards the oxidation of 100 nM NO_2^- and reduction of

Table 1
Simultaneous measurement of NO_2^- and NO_3^- in human plasma using the proposed bienzymatic biosensor and colorimetric assay kit.

Samples	Bienzymatic biosensor		Colorimetric assay kit	
	Conc. of NO_2^- ± SD (nM mL^{-1})	Conc. of NO_3^- ± SD (μM mL^{-1})	Conc. of NO_2^- ± SD (nM mL^{-1})	Conc. of NO_3^- ± SD (nM mL^{-1})
1	492 ± 3.0	20.80 ± 1.1	485 ± 4.0	19.40 ± 2.0
2	594 ± 3.0	19.75 ± 1.3	587 ± 2.0	18.75 ± 1.7
3	583 ± 5.0	19.26 ± 1.0	574 ± 5.0	18.50 ± 3.0
4	518 ± 4.3	14.40 ± 1.2	507 ± 3.5	13.24 ± 2.2
5	390 ± 2.4	9.40 ± 1.4	385 ± 2.2	9.20 ± 1.9
6	485 ± 6.0	16.95 ± 1.1	477 ± 4.0	16.45 ± 1.7

300 nM NO_3^- showing the SD of 3.57% and 2.98% respective for NO_2^- and NO_3^-. Thus, it confirms that the NaR–SOD1–CNT–PPy–Pt electrode is reproducible.

3.9. *Measurement of* NO_2^- *and* NO_3^- *in Human plasma, whole Blood and saliva*

In human plasma, blood and saliva samples, proteins and various co-existing biological substrates are also present. They are perhaps non-specifically adsorbed onto the biosensor electrode surface and cause the adverse reactions such as coagulation, complement activation, platelet adhesion, and leukocyte adhesion. It possibly leads to electrode fouling and hence affects the current response of the biosensor. Therefore, in order to prevent electrode fouling and to achieve more selective NO_2^- and NO_3^- measurements, CA membrane coated bienzymatic biosensor was used. Prior to measurement, the above samples were diluted 10 times with 0.1 M PBS (pH 7.0) in an electrochemical cell. Then, the CV was performed for the plasma samples (Fig. S9) and the current responses at +0.8 V and −0.76 V were observed simultaneously. After that, the concentrations of NO_2^- and NO_3^- were calculated by interpolating the obtained current response into the calibration plot prepared by the NO_2^- and NO_3^- standard solutions and the obtained results were shown in Table 1. Each reading represents the average of three measurements. Further, the measured values were validated by comparing the results obtained using NO_2^-/NO_3^- colorimetric assay kit by Cayman chemicals, Ann Arbor, MI, USA (Cat. no. 780001). The mean ± standard deviation (SD) of 510.3 ± 3.9 nM NO_2^- and 16.76 ± 1.2 μM NO_3^- were obtained in plasma and these values were comparable with the previous reported data (Kage et al., 2000; Tsikas. 2007). Fig. S10 shows the typical CV responses obtained for the bienzymatic biosensor in saliva samples. The concentrations of NO_2^- present in blood and saliva samples were estimated as described above and the results were shown in Table S2. The reported bienzymatic biosensor is regularly used at Peptide and Proteomics Division of DIPAS, Delhi to measure plasma NO_2^- and NO_3^- levels of high altitude sojourns. The concentrations of NO_2^- and NO_3^- are higher in asthma conditioned subjects (Ganas et al., 2001) and lower in hypoxia conditioned subjects (Lundberg et al., 2008) than the reported values. Therefore, it could be used as a clinical diagnostic tool for monitoring NO_2^- and NO_3^- in both the cases since the present biosensor have wide linear range from nanomolar to millimolar.

4. Conclusion

Herein, a novel bienzymatic biosensor based on the coimmobilization of SOD1 and NaR on CNT–PPy nanocomposite was successfully developed for the simultaneous determination of NO_2^- and NO_3^-. It shows broad detection range, lower detection limit, good stability and higher sensitivity and specificity. The advantages provided by this bienzymatic biosensor for the estimation of NO_2^- and NO_3^- in human plasma, blood and saliva samples make it an attractive and potential tool to be used for the clinical samples. The only limitation of this biosensor is the large sample size required for the measurements that will be overcome in future by using screen printed modified electrodes.

Acknowledgments

This work was supported by the DIPAS, DRDO, New Delhi, India (Grant no. TC/370/Task-191(CK)/DIPAS/2013) and the Managing Board of Virudhunagar Hindu Nadar's Senthikumara Nadar College (Autonomous), Virudhunagar, Tamil Nadu, India.

Appendix A. Supporting information

Supplementary data associated with this article can be found in the online version at http://dx.doi.org/10.1016/j.bios.2013.08.036.

References

Asav, E., Akyilmaz, E., 2010. Biosensors and Bioelectronics 25, 1014–1018.
Badea, M., Amine, A., Palleschi, G., Moscone, D., Volpe, G., Curulli, A., 2001. Journal of Electroanalytical Chemistry 509, 66–72.
Boo, Y.C., Tressel, S.L., Jo, H., 2007. Nitric Oxide 16, 306–312.
Bredt, D.S., Snyder, S.H., 1994. Annual Review of Biochemistry 63, 175–195.
Butler, A.R., Feelisch, M., 2008. Circulation 117, 2151–2159.
Campuzano, Z., Loaiza, A., Pedrero, M., Villena, F., Pingarron, J.M., 2004. Bioelectrochemistry 63, 199–206.
Fang, Y.I., Ohata, H., Honda, K., 2009. Journal of Pharmacological and Toxicological Methods 59, 153–155.
Gamboa, J.C.M., Pena, R.C., Paixao, T.R.L.C., Bertotti, M., 2009. Talanta 80, 581–585.
Ganas, K., Loukides, S., Papatheodorou, G., Panagou, P., Kalogeropoulos, N., 2001. Respiratory Medicine 95, 649–654.
Geng, R., Zhao, G., Liu, M., Li, M., 2008. Biomaterials 29, 2794–2801.
Guevara, I., et al., 1998. Clinica Chimica Acta 274, 177–188.
Jobgen, W.S., Jobgen, S.C., Li, H., Meininger, C.J., Wu, G., 2007. Journal of Chromatography B, Analytical Technologies in the Biomedical and Life Sciences 851, 71–82.
Kage, S., Kudo, K., Ikeda, N., 2002. Journal of Analytical Toxicology 26, 320–324.
Kage, S., Kudo, K., Ikeda, N., 2000. Journal of Chromatography B, Analytical Technologies in the Biomedical and Life Sciences 742, 363–368.
Kaminskaya, O.V., Zakharova, E.A., Slepchenko, G.B., 2004. Journal of Analytical Chemistry 59, 1091–1096.
Kevil, C.G., Lefer, D.J., 2011. Cardiovascular Research 89, 489–491.
Lowenstein, C.J., Dinerman, J.L., Snyder, S.H., 1994. Annals of Internal Medicine 120, 227–237.
Lundberg, J.O., Weitzberg, E., Gladwin, M.T., 2008. Nature Reviews Drug Discovery 7, 156–167.
Lundberg, J.O., et al., 2009. Nature Chemical Biology 5, 865–869.
Madasamy, T., Pandiaraj, M., Koteswararao, A., Rajesh, S., Kalpana, B., Sethy, N.K., Kotamraju, S., Karunakaran, C., 2013. Advanced Chemistry Letters 1, 2–9.
Madasamy, T., Pandiaraj, M., Santosh, K., Balamurugan, M., Robson, B., Arun Venkatesh, K., Vairamani, K., Kotamraju, S., Karunakaran, C., 2012. Talanta 100, 168–174.
Manea, F., Remes, A., Radovan, C., Pode, R., Picken, S., Schoonman, J., 2010. Talanta 83, 66–71.
Miranda, K.M., Espey, M.G., Wink, D.A., 2001. Nitric Oxide 5, 62–71.
Mohamed, R., Campbell, J.L., White, J.C., Dimeski, G., 2012. Clinical and Translational Medicine 5, 1–19.
Nagababu, E., Rifkind, J.M., 2010. Methods in Molecular Biology 610, 41–49.
Nataliya, B., Andrei, N., 2005. Nitric Oxide 13, 93–97.
Pandiaraj, M., Madasamy, T., Paradesi Naidu, G., Balamurugan, M., Kotamraju, S., Rao, V.K., Kalpna, B., Karunakaran, C., 2013. Bioelectrochemistry 91, 1–7.
Quan, D., Shim, J.H., Kim, J.D., Park, H.S., Cha, G.S., Nam, H., 2005. Analytical Chemistry 77, 4467–4473.
Rajesh, S., Koteswararao, A., Bhargava, K., Ilavazhagan, G., Kotamraju, S., Karunakaran, C., 2010. Biosensors and Bioelectronics 26, 689–695.
Reiter, S., Habermuller, K., Schuhmann, W., 2001. Sensors and Actuators B: Chemical 79, 150–156.
Rocha, J., Angnes, L., Bertotti, M., Araki, K., Toma, H., 2002. Analytica Chimica Acta 452, 23–28.
Schipper, R.G., Silletti, E., Vingerhoeds, M.H., 2007. Archives of Oral Biology 52, 1114–1135.
Shariar, S.M., Hinoue, T., 2010. Analytical Sciences 26, 1173–1179.
Shiddiky, M.J.A., Won, M., Shim, Y., 2006. Electrophoresis 27, 4545–4554.

Sohail, M., Adeloju, S.B., 2008. Sensors and Actuators B: Chemical 133, 333–339.
Sun, Y., Wang, S., 2009. American Journal of Biomedical Sciences 1, 171–177.
Szabo, C., 1996. Brain Research Bulletin 41, 131–141.
Tsikas, D., Suchy, M.T., Mitschke, A., Beckmann, B., Gutzki, F.M., 2012. Methods in Molecular Biology 844, 277–293.
Tsikas, D., 2007. Journal of Chromatography B, Analytical Technologies in the Biomedical and Life Sciences 851, 51–70.
Vitturi, D.A., Patel, R.P., 2011. Free Radical Biology and Medicine 51, 805–812.
Wang, J., 2006. Analytical Electrochemistry, third ed. John Wiley & Sons, New Jersey.
Wang, J., Xu, Y., Chen, X., Sun, X., 2007. Composites Science and Technology 67, 2981–2985.
Wang, X., Dzyadevych, S.V., Chovelon, J.M., Renault, N.J., Chen, L., Xia, S., Zhao, J., 2006. Talanta 69, 450–455.
Worthman, C.M., Stallings, J.F., Hofman, L.F., 1990. Clinical Chemistry 36, 1769–1773.
Zhang, Z., et al., 2009. Biosensors and Bioelectronics 24, 1574–1579.
Zhu, R., Li, G., Huang, G., 2009. Materials and Corrosion 60, 34–39.